

# **High-Resolution Reaction Spectroscopy of S=-1 Hypernuclei**

H. Noumi

*KEK, Tsukuba, Ibaraki 305-0801, JAPAN*

Y. Fujii, O. Hashimoto, and T. Takahashi

*Tohoku University, Sendai, Miyagi 980-8578, JAPAN*

T. Fukuda and P. K. Saha

*Osaka Electro-Communication University, Neyagawa, Osaka, JAPAN*

## **1 High-resolution Hypernuclear Spectroscopy**

Through precision spectroscopy of the hypernuclear structure, the mechanism of the baryon-baryon interactions and the manner of baryon many-body system can be investigated in the framework of  $SU_F(3)$ . High-resolution spectroscopy opens a new frontier in hypernuclear physics. Recent progress provided by the super-conducting kaon spectrometer SKS should be particularly remarkable. In fact, SKS demonstrated a lot of new features of hypernuclei with its high resolution of better than 2 MeV in FWHM, and brought new questions arising from the unexpected results, as mentioned in Appendix A. The energy resolution of hypernuclear spectroscopy is now stepping up to the level of sub-MeV in  $(e, e'K^+)$  in TJNAF-CEBAF, as is mentioned in Section 3. The same or better level of the energy resolution in J-PARC has to be desired. Therefore, we propose to proceed **high-resolution reaction spectroscopy of hypernuclei at the level of a 200-keV energy resolution** in order to resolve the questions and explore exciting new precision world of hypernuclei. A design of the beam line and spectrometer system for this purpose have been reported elsewhere [1], and the specification is summarized in appendix B.

Here, we stress advantages of the present high-resolution reaction spectroscopy;

- 1) high production rate of hypernuclei enables a series of systematic measurements in reasonably short period.
- 2) Particularly, hyperon-binding energies of the ground and excited states including particle-unbound states or ones with small production cross section could be measured.

One may mind spectroscopy with germanium gamma-ray detector. There is no doubt that its superior performance in resolution is quite powerful in many (hyper)nuclear spectroscopic investigations, as proposed in another part of this letter of intent. However, unfortunately it often requires to produce large amount of hypernuclei in order to compensate its low detection efficiency. In general, many of hypernuclear states are produced at the particle-unstable states. There are many interesting features in such states, as introduced below. Therefore, the high-resolution reaction spectroscopy is necessary and plays a complimentary role of high-resolution

gamma-ray spectroscopy with germanium detectors.

Below, we introduce some typical experimental programs to show the feasibility of the high-resolution spectroscopy with proposed high-resolution beam line. A prospect of the high-resolution spectroscopy to be proceeded in J-PARC will be mentioned at the end.

## 2 Experimental Programs

### 2.1 Fine structure of $\Lambda$ -single particle potential

#### 2.1.1 Motivation

It is one of main purposes in hypernuclear physics to know details of the mean field potentials of nuclear matter with hyperons. We know the magic number of ordinary nuclei is characterized by the spin-orbit potential. In lambda hypernuclei, however, the magnitude of the spin-orbit potential is still unclear. In the p-shell hypernuclei, it is suggested that the  $\Lambda N$  spin-orbit interaction is much (a several times) smaller than the  $NN$  one. On the other hand, fairly large splitting was observed in the  $\Lambda$ -shell orbital state of  ${}^8_9\Lambda\text{Y}$ . If the splitting is due to the  $\Lambda$ -spin-orbit potential, there is a discrepancy on the spin-orbit interactions in light and heavy system. In the spectrum, one can see sizable strength around the splitting states, which could be significant contributions from  $\Lambda$  states coupled to deeper neutron-hole states. In order to obtain the conclusive result, **further decomposition of the spin-orbit splitting states** from the core-excited states is necessary. Namely, much higher-resolution spectroscopy is required to resolve fine structure of the spectrum. The high-resolution beam line is thus indispensable.

#### 2.1.2 Expected spectrum

Fig. 1 shows a simulated excitation energy spectrum produced via the  $(\pi^+, K^+)$  reaction on  ${}^{90}_{\Lambda}\text{Zr}$ , based on the theoretical calculation with Wood-Saxon + S.O. type one-body potential. Here, the momentum resolutions for the beam line and the spectrometer are assumed to be both  $10^{-4}$ . The energy straggling effect is taken into account due to the finite target thickness,  $1\text{mm}(0.653\text{g}/\text{cm}^2)$  of zirconium. The energy resolution of **300 keV** in FWHM is achievable. The spin-orbit splitting states for  $f_{\Lambda}$  and  $d_{\Lambda}$  are clearly separated. Even for  $p_{\Lambda}$  may be decomposed. The core-excited states are expected to be broader due to their intrinsic widths, thus could be distinguished.

#### 2.1.3 Yield estimation

According to the measurement for  ${}^8_9\Lambda\text{Y}$  [2], the ground state of  ${}^9_0\Lambda\text{Zr}$  is expected to be  $0.6 \mu\text{b}/\text{sr}$ . It is well agreed with the theoretical calculation [3]. Below is shown estimated production rate for the ground state in second:

$$\begin{aligned} \text{Rate(cps)} &= I_{Beam}(\text{cps}) \times N_t(\text{cm}^{-2}) \times \frac{d\sigma}{d\Omega}(\mu\text{b}/\text{sr}) \times \Delta\Omega(\text{sr}) \times 10^{-30}(\text{cm}^2/\mu\text{b}) \times \varepsilon_{K^+} \\ &= 10^9 \times \frac{0.1 \cdot 6.53}{90} \cdot 6.022 \times 10^{23} \times 0.016 \times 0.6 \times 10^{-30} \times 0.1 \end{aligned}$$

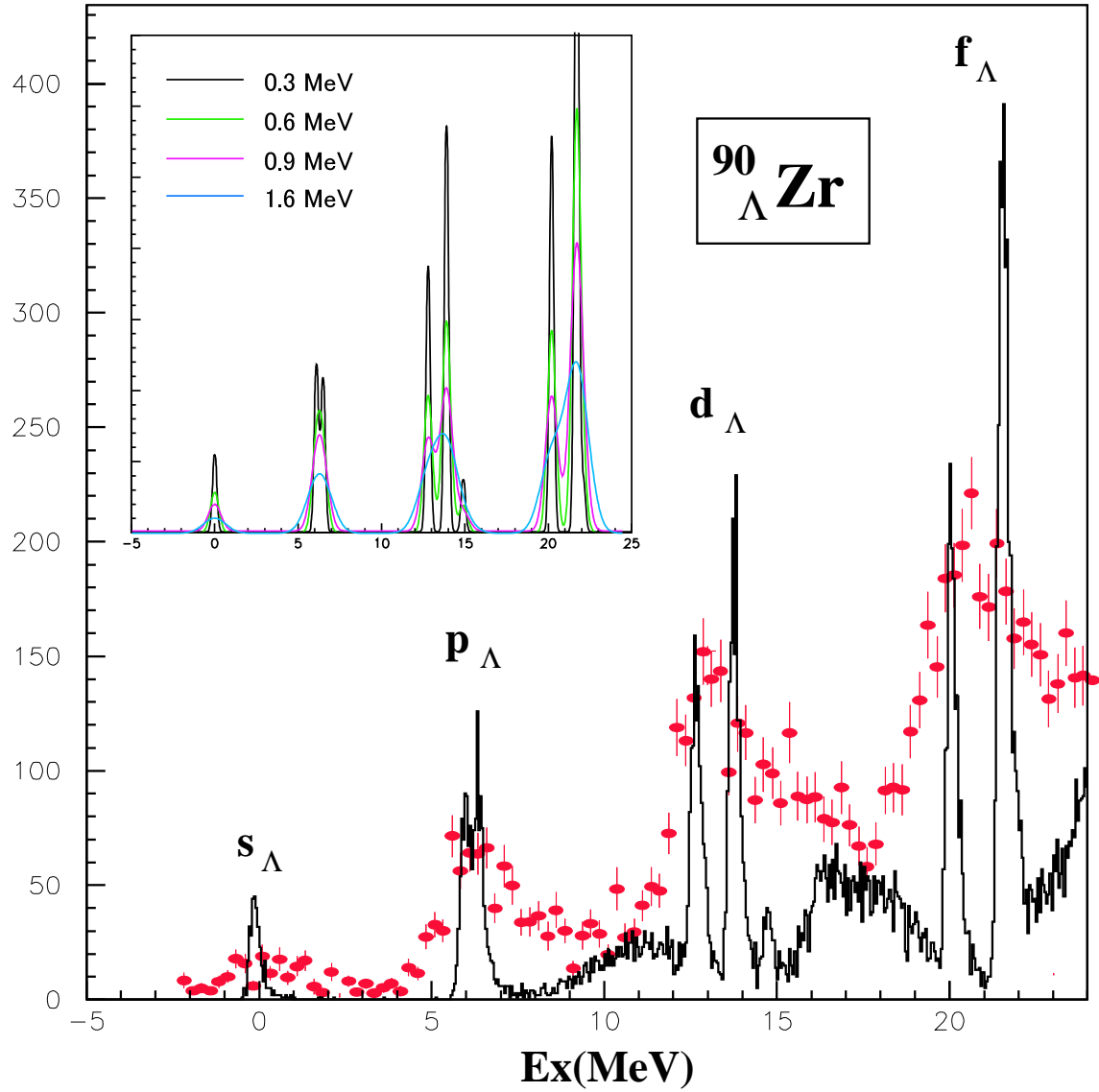


Figure 1: Simulated excitation energy spectrum for  ${}^{90}_{\Lambda}\text{Zr}$  (histogram), together with the measured spectrum for  ${}^{89}_{\Lambda}\text{Y}$  (plot with closed circles). More realistic simulation was made with the Zr target of 1mm thickness, assuming the beam line and spectrometer resolution of  $10^{-4}$  each. Change of the spectrum shape with respect to the energy resolution is also displayed at the up-left corner.

$$= 0.004,$$

where  $I_{Beam}$  and  $N_t$  are beam intensity per second and the number of target, respectively.  $\Delta\Omega$  and  $\varepsilon_{K^+}$  are the solid angle of the kaon spectrometer and the kaon survival rate with respect to the kaon flight length of 12.4m, being 16 msr and 0.1, respectively. The kaon spectrometer requires the tracking devices only at the focal plane. Thus, their efficiency should be taken into account, which is expected to be 0.8. Kaon identification may be one of the key issue in the present system. The most probable and usual way is to reconstruct the mass from measured momentum and beta (time of flight). In the case, the mass resolution is determined almost only by the resolution of beta. Taking the time resolution of 0.2ns, we estimate expected mass resolution to be as good as 20 MeV/c<sup>2</sup>, even when the flight length is set to be 1m. Taking  $3\sigma$  for the kaon mass gate width, the contamination would be less than 1-10 $\sigma$ . Thus, sufficiently good resolution is expected to separate kaons from pions and protons. However, measurement of the time of flight must be done behind the focal place, which sacrifices the kaon survival rate. In case of 1m flight path, another 20% of kaon would be lost.

After all, we have to take into account the kaon detection and identification efficiency of 0.8<sup>3</sup>=0.5, where another factor of 0.8 for DAQ live time is assumed in addition.

In summary, we expect **170 counts/day** for the  ${}^{90}_{\Lambda}\text{Zr}$  ground state (0.6 $\mu\text{b/sr}$ ). This is surprisingly high count rate. Thus, systematic measurements of heavy  $\Lambda$ -hypernuclear structure can be done with high precision in a short period.

## 2.2 Precision spectroscopy of light hypernuclei

### 2.2.1 Motivation

In 1995, core-excited states in  ${}^{12}_{\Lambda}\text{C}$  produced by the  $(\pi^+, K^+)$  reaction were discovered at KEK[4]; two small peaks inbetween well-known two prominent peaks were found. Among two small peaks, for higher one in excitation energy, it is pointed out that a simple configuration of a  $\Lambda$  coupled to a core-nucleus state does not seem to reproduce the excitation energies. Further microscopic treatment in theoretical calculations is required. Recently, an idea of **inter-shell mixed configuration** to describe core excited states is proposed by Motoba *et al.*[5]. In this model, core-nucleus excited states with different parity coupled to the different  $\Lambda$ -orbits can be contributed to describe  $1\hbar\omega$  excited configurations (Fig. 2).

If it is true, a several states with different spin-parity may be populated as core-excited states. In fact, the observed peak looks broader than experimental resolution so that it can be decomposed into two states in peak fitting. Further fine structure of the core-excited states have to be clarified.

### 2.2.2 Yield estimation

In case of  $(\pi^+, K^+)$  on 0.2 g/cm<sup>2</sup>  ${}^{12}\text{C}$ , for the state with the production cross section of 0.1 $\mu\text{b/sr}$ , one can accumulate 100 counts within a day. Fine structure of different spin-parity states can be investigated very efficiently.

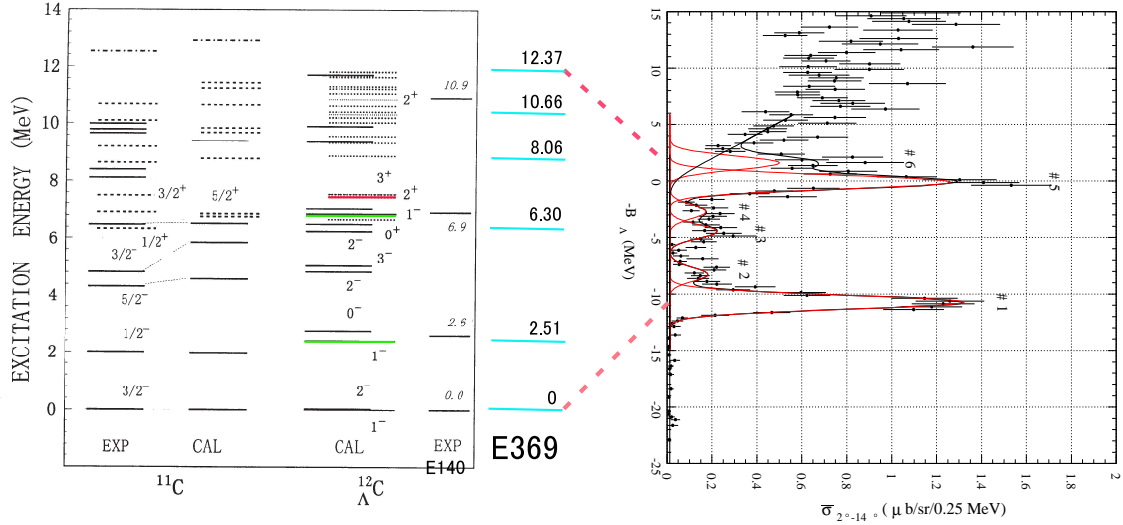


Figure 2:  $^{12}_{\Lambda}\text{C}$  level scheme calculated with an extended model of inter-shell mixed configuration, shown together with the measured spectrum.

## 2.3 Spectroscopy of neutron-rich $\Lambda$ hypernuclei

### 2.3.1 Motivation

Mean field potential for  $\Lambda$  in different nuclear density is of much interest. Precision spectroscopy of  $\Lambda$  hypernuclei with neutron halos would provide information on the  $\Lambda$ -neutron and  $\Lambda$ -neutron-matter interactions. Properties of neutron-halos may be modified to the embedding of a  $\Lambda$  hyperon. D. E. Lansky and his co-workers examined the response of neutron-single particle energy in  $^{12}_{\Lambda}\text{Be}$  with different  $\Lambda N$  interactions [6]. They found the level scheme of neutron-single particle energy is dependent on the strength of  $\Lambda NN$  force, as shown in Fig. 3.

However, two step reaction process must be required to reach neutron-halo  $\Lambda$  hypernuclei. The high-resolution and high-sensitivity is required to investigate such hypernuclei. The high-resolution beam line is thus best-suited for the present purpose.

### 2.3.2 Feasibility

Let us consider the case of  $^{12}\text{C}(\pi^-, K^+)_{\Lambda}^{12}\text{Be}$ . Production cross section could be approximately estimated by taking a product of two single-step cross sections:

$$\begin{aligned} d\sigma/d\Omega|_{(\pi^-, K^+)} &= \sigma(\pi^-, \pi^0)/(\pi R^2) \times d\sigma/d\Omega|_{(\pi^0, K^+)} \\ &\sim 0.3(\text{mb})/300(\text{mb}) \times 0.01(\text{mb/sr}) = 10(\text{nb/sr}). \end{aligned}$$

Here,  $\pi R^2$  represents the cross section of the target nucleus seen by the intermediate  $\pi^0$ . Another two-step process,  $(\pi^-, K^0) \rightarrow (K^0, K^+)$ , could contribute to the production and is expected to be the same order of magnitude. Recent realistic theoretical estimation by Tretyakova *et al.* reported the cross section of 6.5 nb/sr in  $^{12}\text{C}(\pi^-, K^+)_{\Lambda}^{12}\text{Be}(1^-)$ . Taking this cross section and using 0.6g/cm<sup>2</sup> thick carbon target, about **13 counts/day** could be observed.

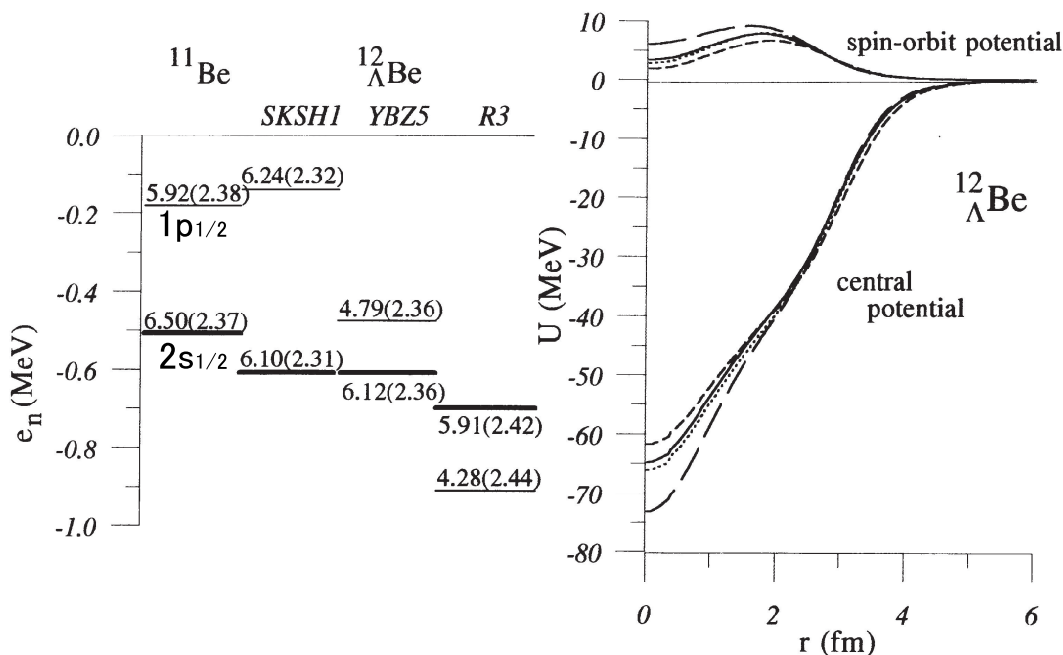


Figure 3: Neutron-single particle energy (left) and potentials (right) calculated with three different sets of  $\Lambda N$  interaction presented by D. E. Lansky [6].

#### Note

Experimental investigations of neutron rich  $\Lambda$  hypernuclei via the double charge exchange reactions are proposed in the different Letter of Intent [7]. The  $\Lambda$ - $\Sigma$  coupling appears in the  $\Lambda NN$  three-body interaction and plays a significant role on the structure of  $\Lambda$  hypernuclei. It is successfully demonstrated that the *coherent and incoherent  $\Lambda$ - $\Sigma$  coupling effects* explain the binding energies of all the s-shell hypernuclear bound states [8], solving so-called long-standing “overbinding problem” [9]. This unique phenomenon has to be studied in p-shell or other  $\Lambda$  hypernuclei. We discussed in the Letter that spectroscopic studies of neutron rich  $\Lambda$  hypernuclei in light system provide opportunities to examine the *coherent  $\Lambda$ - $\Sigma$  coupling effect*. It is predicted that the *coherent  $\Lambda$ - $\Sigma$  coupling effect* causes the *coherent  $\Lambda$ - $\Sigma$  mixing* in neutron matter, which is strongly related to the hyperon composition of neutron-star matter [10]. The present high-resolution beam line is requested to proceed the spectroscopic studies of neutron rich  $\Lambda$  hypernuclei.

## 2.4 Spectroscopic study of $\Sigma$ -nucleus potential

### 2.4.1 Motivation

In order to understand the baryon-baryon interactions not only in free space but also in baryonic matter in extended flavor space, it is necessary to investigate nuclei including other octet-strange baryon(s) like  $\Sigma$ ,  $\Xi(\Lambda\Lambda)$ , and so on. In particular, the  $\Sigma N$  interaction is important and closely related to the  $\Lambda N$  interaction through mixing since  $\Sigma$ 's mass differs only 80

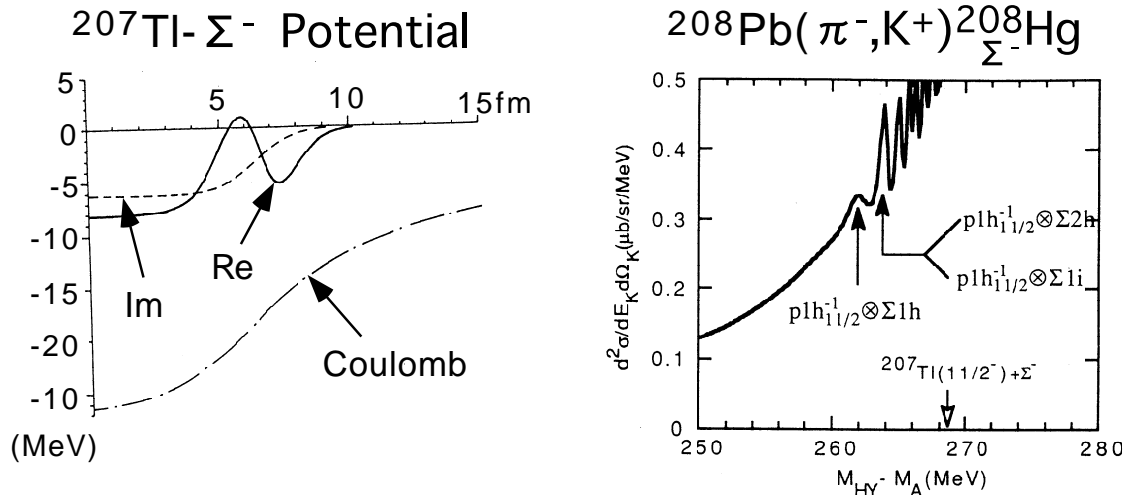


Figure 4: (left) Calculated  $\Sigma$ -Tl potential and (right)  $^{208}_{\Sigma^-}\text{Hg}$  spectrum produced by the  $(\pi^-, K^+)$  reaction.

MeV from  $A$ 's. We wish to proceed the  $\Sigma$ -hypernuclear study as well as the  $\Lambda$ -hypernuclear study.

Recently, a role of strangeness in high-density nuclear matter, such as neutron stars or supernovas, has been intensively discussed. For example, it is said that the admixture of hyperons in a neutron star makes the equation of state (EOS) soften. As a result, the maximal mass of neutron star becomes smaller than that in case of no hyperon admixture. This may change a formation scenario of a neutron star and blackhole and the thermal and structural evolution of a neutron star. Above arguments are strongly related to the hyperon-nucleon and hyperon-hyperon interactions in nuclear medium. Particularly, behaviours of three body forces may affect the EOS. a  $\Sigma$  hyperon is expected to appear first in dense nuclear matter due to its negative charge.  $\Sigma$  also plays a key role on the three body forces through the  $\Lambda$ - $\Sigma$  coupling effect. In this regards, it is of particular importance to investigate the  $\Sigma$ -nucleus potential through spectroscopic study of  $\Sigma$  hypernuclei.

#### 2.4.2 $\Sigma$ -nucleus bound state

As is mentioned in Appendix A, it is demonstrated that the  $\Sigma$ -nucleus potential is strongly repulsive in medium to heavy nuclei. This information is brought by the analyses of the inclusive  $(\pi^-, K^+)$  spectra. To investigate the  $\Sigma$ -nucleus potential further, its nature at the nuclear surface is necessary. With the assist of the Coulomb potential, one may observe the narrow peak structure of deeply bound  $\Sigma^-$ -atomic states or so-called the **Coulomb-Assisted Hybrid  $\Sigma$ -hypernuclear Bound States (CAHBS)**. Fig. 4 shows calculated  $^{208}_{\Sigma^-}\text{Hg}$  spectrum produced by the  $(\pi^-, K^+)$  reaction [11]. According to theoretical calculation, the  $^{208}_{\Sigma^-}\text{Hg}$  [ $p_{h11/2}^{-1}, \Sigma_{1h}$ ] an [ $p_{h11/2}^{-1}, \Sigma_{1i}$ ] states may be populated by the  $(\pi^-, K^+)$  reaction, which are 2 MeV apart from each other and have the widths of 1.6 MeV and 0.2 MeV, respectively. Utilizing the high-resolution beam line, these states can be seen. Detailed information on the  $\Sigma$ -nucleus potential could be extracted.

### 2.4.3 Yield estimation

The cross section of CAHBS is expected to be as small as  $0.1\mu/sr$ . Since the wave function of the state is defusing out of the nucleus, the overlapping of the wave with the nuclear core becomes small. This causes the state width due to absorption small but also makes the production cross section small.

Expected yield is estimated to be about **10 counts/day**, for the lead target of  $0.6g/cm^2$ . This count rate is sufficiently high, and hence, the experiment could be carried out within reasonably short period.

## 3 Impact for Other Facilities in the World

At present, there is no facility, other than TJNAF, which has and demonstrates any hypernuclear production systems with high-resolution at the level of sub-MeV. TJNAF-CEBAF provides high-quality electron beam up to 6 GeV, and hence, enables to carry out high-resolution spectroscopic investigations via the  $(e, e'K^+)$  reactions. Their high-precision hypernuclear excitation spectra are being available.

Since the  $(e, e'K^+)$  reaction involves the charge transfer of  $\Delta Z=-1$ , neutron-rich  $\Lambda$  hypernuclei can be produced. Using the nuclear target of isospin equal to 0, one can investigate mirror hypernuclei of those obtained via the  $\Delta Z=0$  reaction like  $(\pi^+, K^+)$ . To compare both the  $(\pi^+, K^+)$  and  $(e, e'K^+)$  spectra and to obtain information from mirror hypernuclei, we need at least the same level of the energy resolution to that achieved at TJNAF.

## 4 A Prospect for High-Precision Hypernuclear Spectroscopy

The high-intensity pion beam allows us to carry out **hypernuclear decay spectroscopy with high precision**. In this beam line, the differential decay widths ( $d\Gamma/dE$  and  $d\Gamma/d\theta$ , energy and angular distributions) in addition to  $\Gamma$  can be measured very precisely, based on high statistics.

The **nonmesonic decay mechanism** of hypernuclei has yet to be revealed. There exists a discrepancy between theory and experiment on the decay branching ratios in nonmesonic process. However, available data seem poor in quality. Recently, new observables, the asymmetry of nonmesonic decay has been measured. A further accumulation of data with better quality is necessary. Precise measurements of the decay observables will improve the situation.

**Mesonic decay in heavy hypernuclei** is sensitive to pion propagation in the nucleus, which reflects the dynamics of hadrons in the nuclear medium. **Exotic decay**, such as positive pion emission, is interesting since it is sensitive to the  $\Lambda\Sigma$  mixing effect. The sensitivity for the branching ratios of these decays will be as high as  $10^{-3}$  in the present beam line.

Various contributions to the weak decay mechanism will be clarified through the high-statistics, high-sensitivity hypernuclear decay spectroscopy.



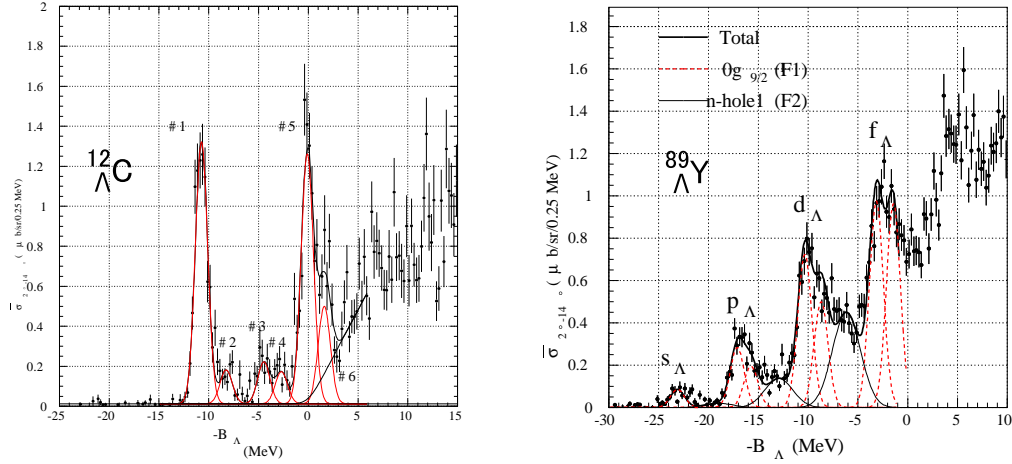


Figure 5:  ${}_{\Lambda}^{12}\text{C}$  (left) and  ${}_{\Lambda}^{89}\text{Y}$  (right) spectra produced by the  $(\pi^+, K^+)$  reactions, observed with SKS.

The **hypernuclear magnetic moment** is quite sensitive to the details of the hyperon-nucleon interaction in the nuclear medium. Particularly, the isospin dependence is interesting since it would reflect the structure of the exchange current, *e.g.*, the contributions of kaon exchange and/or  $\Sigma$  excitation. It has been an ambitious dream to measure the hypernuclear magnetic moment. This dream may come true at the present facility.

## Appendix A: Brief Description on Hypernuclear Spectroscopy with SKS

Recent progress on hypernuclear investigations provided by the super-conducting kaon spectrometer SKS shows importance of high-precision spectroscopy for hypernuclear physics. Here, we describe briefly what we learned with SKS.

First, the single-particle nature of  $\Lambda$  hypernuclei was clearly shown by  $\Lambda$ -major shell structures measured by the  $(\pi^+, K^+)$  reactions. A series of  $\Lambda$ -major shell orbital states from the ground to highly-excited states were clearly observed even in heavy hypernuclei of the mass number up to 208, owing not only to the selectivity of the  $(\pi^+, K^+)$  reaction but also to the high resolution. Observed  $\Lambda$ -major shell orbital states in  ${}_{\Lambda}^{89}\text{Y}$  were found to be decomposed into two peaks (Fig. 5-right). These states were first claimed to be  $\Lambda$  spin-orbit splitting states. This result seemed to indicate the large spin-orbit term in  $\Lambda$ -single particle potential, in contrary to the other suggestion in light hypernuclear system where small  $\Lambda N$  spin-orbit interaction is favored. The configuration of the observed states is still unclear since significant contribution from hole states of the core nucleus has to be taken into account.

Second, SKS found unique quantum states in hypernuclei. Supersymmetric states were observed in  ${}_{\Lambda}^9\text{Be}$ , in which a  $\Lambda$  hyperon can occupy a unique orbital configuration since  $\Lambda$  is free from Pauli exclusion principle of the nucleon. A discovery of core-excited states in  ${}_{\Lambda}^{12}\text{C}$  was surprisingly provided since their excitation energies were never reproduced with a naive picture

of a  $\Lambda$  coupled to core- $^{11}\text{C}$  excited states (Fig. 5-left). This is an example of unexpected and interesting results brought by the high-precision spectroscopy of hypernuclei. A unique idea of configuration-mixed states is proposed to solve the problem. The mode allows a mixture of different  $\Lambda$ -major orbital states coupled to core- $^{11}\text{C}$  excited states.

Third, SKS opened a new window to investigate hypernuclei via the double charge exchange reactions,  $(\pi^-, K^+)$ . One can create a  $\Sigma^-$  hyperon in a nucleus by the  $(\pi^-, K^+)$  reaction. We demonstrated a strongly repulsive sigma-nucleus potential from the analyses of the  $(\pi^-, K^+)$  inclusive spectra on medium to heavy nuclei [13]. The  $(\pi^-, K^+)$  reaction is one of ways to produce a neutron-rich  $\Lambda$ -hypernucleus. Although the production rate of  $\Lambda$ -hypernucleus via  $(\pi^-, K^+)$  is typically two or three orders of magnitude less than that via  $(\pi^+, K^+)$ , an experiment was carried out to observe  $^A_-\text{Li}$  by the  $(\pi^-, K^+)$  reaction on  $^{10}\text{B}$  [14].

## Appendix B: High-Resolution GeV-Pion Beam line

The main proton synchrotron of J-PARC will deliver a high-power beam of 50 GeV and 15  $\mu\text{A}$ . By taking advantage of the low-emittance primary beam, a **High-Intensity, High-Resolution GeV-Pion Beam Line** can be designed. The beam line will provide a pion intensity as high as  $10^9$  per second and a momentum resolution as good as  $10^{-4}$ , which are respectively 1000-times more and 10-times better than those realized at K6 of the KEK 12-GeV PS [12]

The present beam-line facility will enable us to increase the production rate of hypernuclei drastically, and will provide us a so-called hypernuclear factory with the  $(\pi, K^+)$  reaction. The  $(\pi, K^+)$  reaction has unique features; 1)it favors to populate stretched states, 2)can produce polarized hypernuclei, and 3)is a background-free reaction. The  $(\pi, K^+)$  reaction plays a complementary role on the hypernuclear study to the  $(K^-, \pi)$  reaction. Thus, the pion beam line should be constructed. Utilizing the present facility, next-generation hypernuclear studies with high precision will be proceeded at J-PARC, where **high resolution, high statistics, and high sensitivity** will be key issues.

A layout of the proposed beam line is illustrated in Fig. 6, together with a kaon spectrometer. The beam line consists of two halves. The first half is from PP to MS and for separating pions from the other secondary particles with an electrostatic separator. Since no tracking devices are available, due to the high counting rate, the beam momentum must be determined by measuring the reaction point where the beam position is strongly correlated with its momentum. Thus, the second half is from MS to FF and for making the beam dispersive vertically at FF. The dispersion and vertical magnification at FF are to be  $\sim 10\text{cm}/\%$  and  $-0.4$ , respectively. A momentum resolution of  $10^{-4}$  can be achieved when the source size (production target) is smaller than 2.5mm.

The total length and acceptance of the beam line are **35m** and **4msr $\cdot\%$** . According to the Sanford-Wang formula [15] the  $\pi^+$  intensity is estimated to be more than  $10^9$  per second with a platinum production target 6cm long.

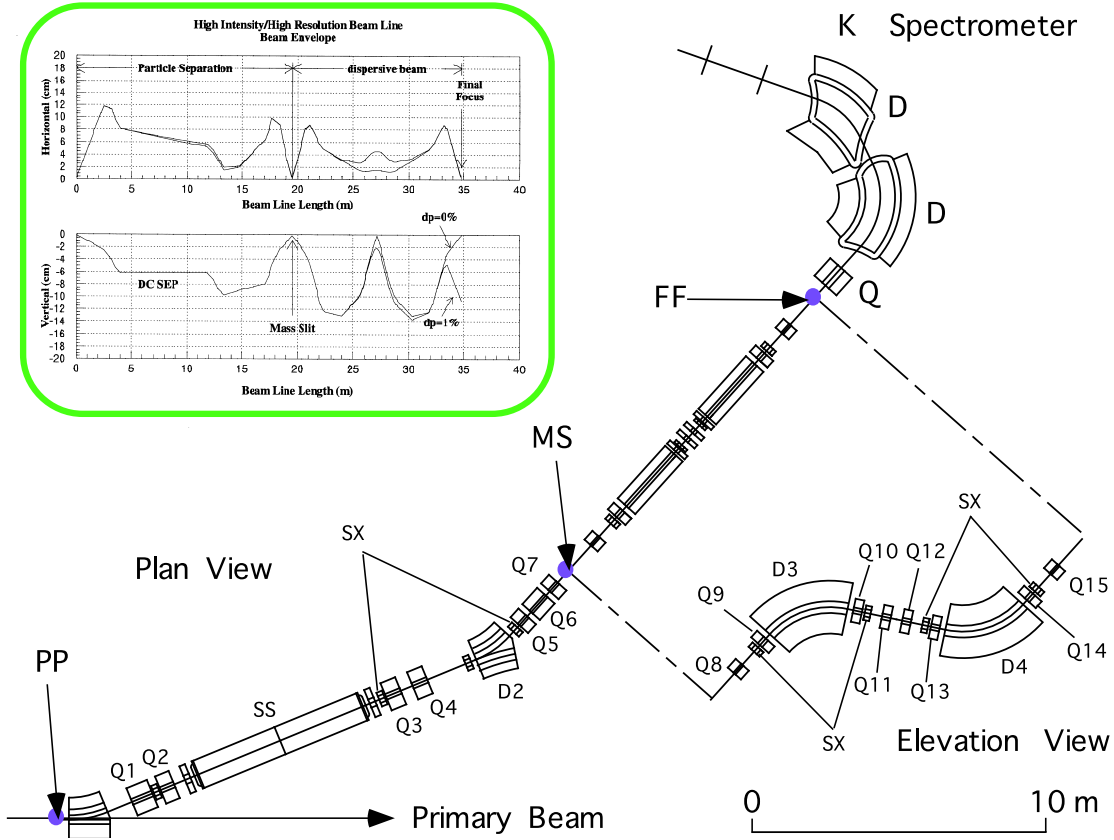


Figure 6: High-intensity, high-resolution pion beam line and kaon spectrometer.

The kaon spectrometer in the figure is designed to be a resolution as good as  $10^{-4}$  to match with the pion beam line. This is obviously optimized for the resolution, compromising with the acceptance and kaon survival rate. The specifications of the kaon spectrometer should be changed, if necessary, so that the resolution, acceptance, maximum central momentum, total length, cost, and so on, will have to meet experimental requests.

The design concept of the kaon spectrometer is summarized as follows.

1. The kaon momentum is determined by the hit position at the focal plane. The resolution is almost determined by the horizontal beam size at the experimental target.
2. The vertical vertex point can be reconstructed from the vertical position and divergence at the focal plane. The vertex resolution of less than 1mm is thus required so that the beam momentum resolution is to be  $10^{-4}$ , which is predominantly determined by the primary beam size at the production target.
3. Satisfying items 1 and 2, we could remove any vertex detectors at around the target, where the counting rate is expected to be too high to drive counters.

We could design a kaon spectrometer to meet above conditions. The horizontal magnification and dispersion are  $-0.851$  and  $8.327$  cm/%, respectively. The vertical magnification ( $R33$ ) is  $-3.08$ . Since the spectrometer has a vertical focus, the vertex resolution is determined by

$Y_O=Y_I/R33\sim 0.5\text{mm}/3.08\sim 0.16\text{mm}$ ;  $\pm 1\text{mm}$ , where  $Y_O$  and  $Y_I$  represent the vertex resolution (object size) and position resolution (image size) at the focal plane, respectively.

Specifications of the pion beam line and kaon spectrometer are summarized in Table 1.

Table 1: Specifications of the pion beam line and kaon spectrometer. <sup>a)</sup> Corrections for higher order aberrations are required.

	$\pi$ Beam Line	K Spectrometer
Max. Central Momentum(GeV/c)	1.5	1.5
Total Length(m)	34.738	12.4
Horizontal Acceptance(mrad)	$\pm 50$	$\pm 100$
Vertical Acceptance(mrad)	$\pm 10$	$\pm 40$
Momentum acceptance(%)	$\pm 1$	$\pm 5$
Horizontal Magnification	0.773	-0.851
Vertical Magnification	-0.409	-3.084
Dispersion(cm/%)	10.614	8.327
Momentum Resolution( $\Delta P/P$ )	$10^{-4}$	$10^{-4}$ <sup>a)</sup>

## References

- [1] H. Noumi, Nucl. Phys. **A639**, 117c(1998).
- [2] H. Hotchi, Doctor Thesis, University of Tokyo, (2000).
- [3] T. Motoba, H. Bandō, R. Wünsch, and J. Žofka, Phys. Rev. **C38**, 1322(1988).
- [4] T. Hasegawa *et al.*, Phys. Rev. Lett. **74**, 224(1995).
- [5] T. Motoba, Nucl. Phys. **A639**, 135c(1998).
- [6] D. E. Lansky, Nucl. Phys. **A639**, 157c(1998).
- [7] P. K. Saha, T. Fukuda, and H. Noumi, LOI at the 50-GeV PS, 2002.
- [8] Y. Akaishi *et al.*, Phys. Rev. Lett. **84**, 3539(2000).
- [9] R. H. Dalitz *et al.*, Nucl. Phys. **B47**, 109(1972).
- [10] S. Shinmura *et al.*, J. Phys. **G28**, L1(2002).
- [11] S. Tadokoro and Y. Akaishi, Phys. Lett. **B282**, 19(1992).
- [12] The K6-SKS spectrometer system has realized about 50 events of the  ${}^{12}\text{C}(\text{g.s.})$  production per hour with a graphite target 1.8g/cm<sup>2</sup> thick.
- [13] H. Noumi *et al.*, Phys. Rev. Lett. **89**, 072301-1(2002).
- [14] T. Fukuda *et al.*, KEK-PS E521 proposal, 2002.
- [15] J. R. Sanford and C. L. Wang, BNL 11279 and BNL 11479 (1967); C. L. Wang, Phys. Rev. Lett., **25**, 1068 (1970).